16

逆問題の CFD-EFD 相互検証への適用

鄭 信圭[1]

Application of inverse method to mutual verification of CFD-EFD

Shinkyu Jeong[1]

Abstract

Inverse method is applied to geometry estimation of wind tunnel models. By defining the pressure distribution obtained from wind tunnel test as the target of inverse method, approximate geometry estimation is possible. The inverse method used in this paper is based on Takanashi's concept that utilizes integral equations and 'residual-correction' technique. Geometry of two wind tunnel models were estimated. One is 23.5% scale and the other is 8.5% scale of NEXST-1(National Experiment Supersonic Transport). The deviation of the estimated value from the original CATIA geometry was within a reasonable order if manufacturing limitation is considered. The geometry of the 8.5% scale wind tunnel model was measured for validation by using a non-contact three-dimensional measuring device employing laser beam and auto-focus system. The result shows the validity of the present method for approximate geometry estimation.

Introduction

National Aerospace Laboratory (NAL) in Japan started a scaled supersonic experimental aircraft program called NEXST[1)] in 1996 to establish advanced design technologies for the next generation supersonic transport. This program is comprised of development of two types of unmanned experimental aircraft, a non-powered (NEXST-1) and a twin-jet engine airplanes (NEXST-2). The design tools incorporated in these aircrafts are as follow:

1) Carlson's method[2)] for warp design
2) Area-Rule and Adjoint method for fuselage design[3)]
3) Inverse method for NLF[4)] (Natural Laminar Flow) wing design

The following flight tests will ensure the validity of these design techniques. Before flight test, a lot of wind tunnel tests and CFD analysis for NEXST configurations were conducted to predict its performance.

In the 3rd SST-workshop held in Dec. 2001, many researchers supplied the CFD analysis results of NEXST-1 using their own CFD-code. These results were compared with those of wind tunnel tests. As a whole, they show a good agreement with each other. However, the pressure distributions near 50% spanwise section, where the leading edge kink is located, show some discrepancies in the leading edge region. The pressure distribution obtained from wind tunnel test has a somewhat large peak at leading edge region, as shown in Fig. 1.

Such a large peak at leading edge means that transition occurs from the leading edge. As a result, NLF region will never appear on the designed wing surface.

Possible reasons of this discrepancy are as follows:

CFD side

1) Coarse resolution in computational grid and lack of convergence
2) Turbulence model and transition location
3) Aeroelastic deformation

Wind tunnel test side

1) Deviation from original CATIA geometry due to limitation during manufacturing
2) Lack of experimental repeatability
3) Using roughness to forced transition

In this investigation, the geometric deviation of the NEXST-1 wind tunnel model from the original CATIA data is estimated by inverse method. By defining the pressure distribution from wind tunnel test as the target for inverse method, the corresponding geometry is obtained. In this study, two different scales of NEXST-1's wind tunnel models were used for validation. One is 23.5% scale model, which is intended for transition characteristics measurement and the other is 8.5% scale model, for force and pressure measurement. In the case of 8.5% scale wind tunnel model, three-dimensional non-contact geometry measurement was also conducted. The geometry of original CATIA data, inverse estimation, and

[1] National Aerospace Laboratory, JAPAN
7-44-1, Jindaiji-Higashi, Chofu, Tokyo, 182-8522
E-mail: Jeong@nal.go.jp

three-dimensional measurement were compared. The result shows the validity of the present method for approximate geometry estimation.

Inverse method

The inverse method employed in this investigation is based on Takanashi's concept[5] that uses integral equations and 'residual-correction' technique. The procedure typical to this inverse method is shown in Fig.2.

1) Arbitrary initial wing geometry and the target pressure distribution are input.
2) Flow analysis around the initial wing geometry is performed, and the difference between the objective and the target pressure distribution is calculated.
3) From this difference, the geometry correction is determined by solving integral equations.
4) Adding the geometry correction to the initial wing geometry, new wing geometry is obtained.
5) Routines 2)~4) are iterated until the difference between objective and target pressure distribution become small enough.

The original Takanashi's method is for sub- and transonic flow. The extension to supersonic flow region was done by author. The derived integral equations for supersonic flow[6] are as follows:

The integral equation for thickness correction

$$\Delta u_s(x,y) = -\Delta w_s(x,y) + \frac{1}{\pi}\iint_{\Gamma_1} \frac{(x-\xi)\Delta w_s(\xi,\eta)}{\sqrt{(x-\xi)^2-(y-\eta)^2}^3} d\xi d\eta$$

$$\Delta u_a(x,y) = \Delta\phi_x(x,y,+0) + \Delta\phi_x(x,y,-0)$$

$$\Delta w_s(x,y) = \Delta\phi_z(x,y,+0) - \Delta\phi_z(x,y,-0)$$

The integral equation for camber correction

$$\Delta w_a(x,y) = -\Delta u_a(x,y) + \frac{1}{\pi}\iint_{\Gamma_1} \frac{(x-\xi)\Delta u_a(\xi,\eta)}{(y-\eta)^2\sqrt{(x-\xi)^2-(y-\eta)^2}} d\xi d\eta$$

$$\Delta u_a(x,y) = \Delta\phi_x(x,y,+0) - \Delta\phi_x(x,y,-0)$$

$$\Delta w_a(x,y) = \Delta\phi_z(x,y,+0) + \Delta\phi_z(x,y,-0)$$

Δ means the difference between target and objective. $\Delta\phi_x$ and $\Delta\phi_z$ can be represented as follows:

$$\Delta\phi_x(x,y,\pm 0) = -\frac{1}{2\beta^2}\Delta C_{p\pm}\left(x,\frac{y}{\beta}\right),$$

$$\Delta\phi_z(x,y,\pm 0) = \frac{1}{\beta^3}\frac{\partial \Delta f_\pm(x,y)}{\partial x}$$

where the subscript '$\pm$' denotes the upper and lower surface of the wing and $\beta^2 = M^2 - 1$. The integrated value for thickness correction, however, does not always satisfy closure condition at trailing edge. To settle this problem, Δw_s is modified as follows:

$$\Delta w_s^{\mathrm{mod}}(x,y) = \Delta w_s(x,y) - \frac{\int_{L.E.}^{T.E.} \Delta w_s(\xi,y)d\xi}{\ell}$$

where l is local chord length and $\overline{dx}$ is chord length divided by the number of panels at each spanwise location. The geometry correction can be computed by performing the numerical integration in the x-direction.

$$\Delta f_\pm(x,y) = \frac{1}{2}\int_{L.E.}^{x} \Delta w_a(\xi,y)d\xi \pm \frac{1}{2}\int_{L.E.}^{x} \Delta w_s^{\mathrm{mod}}(\xi,y)d\xi$$

Results

The verification of the present method was performed with two different scales of NEXST-1's wind tunnel models. One is 23.5% scale and the other is 8.5% scale. In both cases, the largest discrepancy between pressure distribution from CFD analysis and that from wind tunnel test was located at 50% spanwise section. The discrepancies in spanwise regions less than 30% and more than 70% were negligible compared to that of 50% spanwise section. Thus, the target pressure distribution of inverse estimation was defined as follow:

1) In spanwise regions less than 30% and more than 70% : Pressure distribution from CFD analysis is set to be equal to the target pressure distribution
2) In spanwise region 30% and 70%: Using pressure distributions at 30%, 50% and 70% spanwise sections obtained from wind tunnel test, pressure distributions of internal sections are interpolated.

Figure 3 shows the target pressure distribution for inverse estimation. The inverse estimation was then performed using the defined target pressure distribution and CFD geometry as an initial wing.

Case1: 23.5% model

Figure 4 compares the target pressure distributions to that of CFD geometry, and that of the geometry obtained by inverse method after 4 iterations. The pressure distribution of the geometry obtained by inverse method approached that of the target very closely. Figure 5 shows the geometry corresponding to each pressure distribution. The maximum thickness deviation at leading edge region is about –0.4mm, which is 0.094% decrease compared with CFD geometry. This deviation is somewhat large. However, in this case, inverse method was iterated without any geometry constraint. Inverse method using integral equation does not have unique solution geometry for designated target pressure distribution. To get the purpose-satisfactory solution geometry, some geometry constraints are necessary.

Case 2: 8.5% model

The geometry estimation of 8.5% scale model was performed with fixed leading and trailing edge constraint. Figure 6 compares the target pressure distribution to that of CFD geometry, and that of inverse method at 50% spanwise section. After 6 inverse iterations, the pressure distribution of the geometry obtained from inverse estimation almost converged to that of target. The corresponding geometry is shown in Fig. 7. The maximum thickness deviation at leading edge region is about 0.1mm, which is 0.06% increase compared to CFD geometry. About 0.1mm's deviation is within the reasonable order if manufacturing limitation is considered. Geometry of 8.5% scale wind tunnel model was measured with three-dimensional non-contact measuring device, as shown in Fig. 8. It is possible to measure the geometry very accurately using this device, which employs laser beam and auto-focus system. Measurement results are shown in Fig. 9. It shows a good agreement with the original CATIA geometry in inboard region. The maximum thickness deviation near the leading edge at 50% spanwise sections is about 0.15mm, an increase of 0.09% compared to the CATIA geometry. However, in outboard region, the discrepancy becomes very large. Figure 10 shows the geometric comparison of CATIA data, inverse estimation, and three-dimensional measurement. Though the estimated geometry does not coincide with that of 3-D measurement perfectly, the deviation values from the original CATIA geometry are almost of the same level. This confirms the validity of the present method in estimating the actual geometry used in wind tunnel experiment.

Concluding Remark

In this study, inverse method is applied to geometry estimation for wind tunnel models. By defining the pressure distribution obtained from wind tunnel test as the target of inverse method, approximate geometry estimation is possible. The geometry of two wind tunnel models of NEXST-1 were estimated, one is 23.5% scale and the other is 8.5% scale. The estimated deviation from the original CATIA geometry was within reasonable order if manufacturing limitation is considered. The geometry of 8.5% scale wind tunnel model was measured for validation by using a non-contact three-dimensional measuring device that can measure geometry with high resolution. The result shows the validity of the present method in estimating model's geometry.

References

1. K. Sakata, "Supersonic Experimental Airplane Program in NAL (NEXST) and its CFD-Design Research Demand," 2nd International Workshop on CFD fort SST, pp. 53-56, Jan., 2000.

2 .H. W. Carlson and W. D. Middleton, "A Numerical Method for the Design of Camber Surface of Supersonic Wings with Arbitrary Planform," NASA TN D-2341, 1964.

3. Y. Makino, T. Iwamiya and Z. Lei, "Fuselage Shape Optimization of Wing-body Configuration with Nacelles," AIAA 2001-2447, 2001.

4. K. Matsushima, T. Iwamiya and W. Zhang, "Inverse Wing Design for Scaled Supersonic Experimental Airplane with Ensuring Design Constraints," 2nd International Workshop on CFD for SST, pp. 91-96, 2000

5. S. Takanashi, "Iterative Three Dimensional Transonic Wing Design Using Integral Equations," *Journal of Aircraft*, Vol. 22, No. 8, pp. 655-660, 1985.

6. S. Jeong, S. Obayashi, K. Nakahashi, K. Matsushima and T. Iwamiya, "Iterative Design Method for Supersonic Wings Using Integral Equations," *Computational Fluid Dynamics Journal*, Vol. 7, No. 3, pp. 356-374, October, 1998.

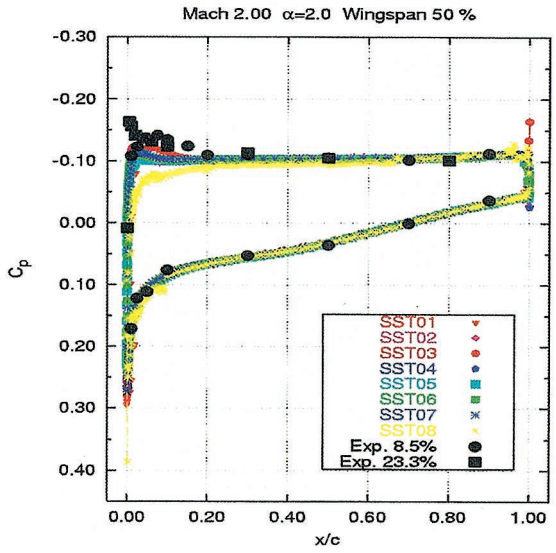

Figure 1. Pressure distributions from CFD analysis and wind tunnel test.

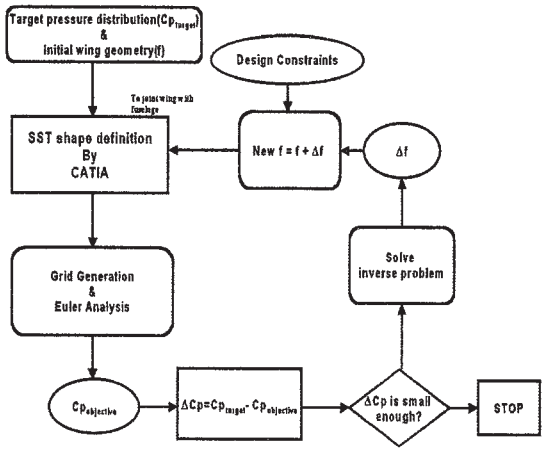

Figure 2. Flow-chart of inverse method

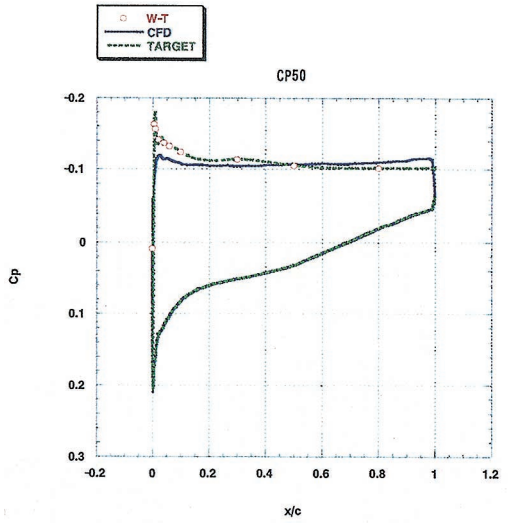

Figure 3. Target pressure distribution for inverse estimation

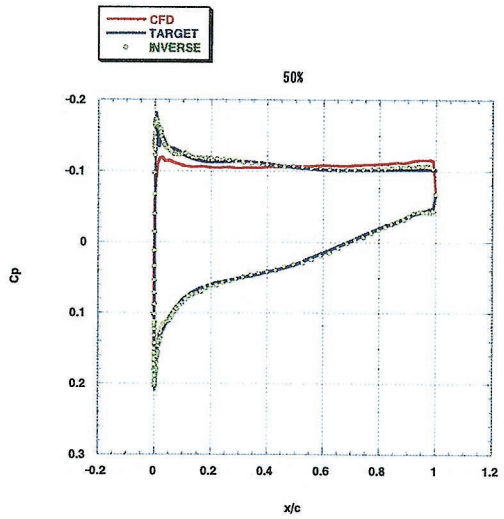

Figure 4. Pressure distribution of geometry of CFD, target, and geometry obtained from inverse method

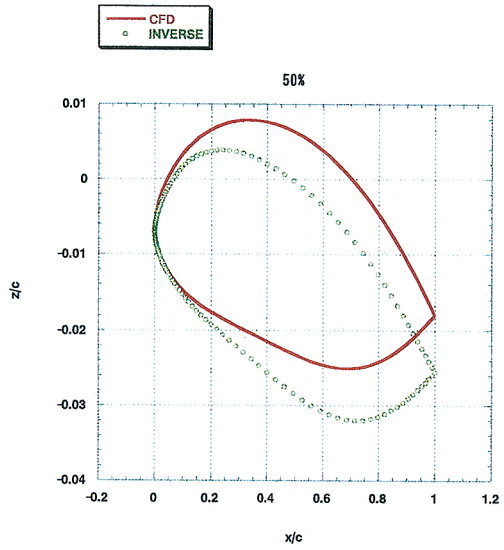

Figure 5. Corresponding geometry of CFD analysis and obtained by inverse method.

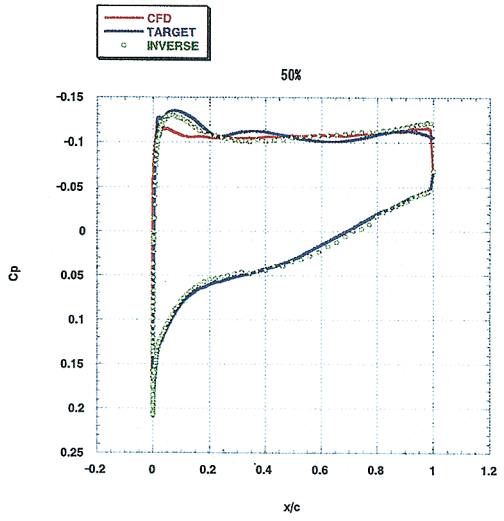

Figure 6. Pressure distribution of geometry of CFD, target, and geometry obtained by inverse method

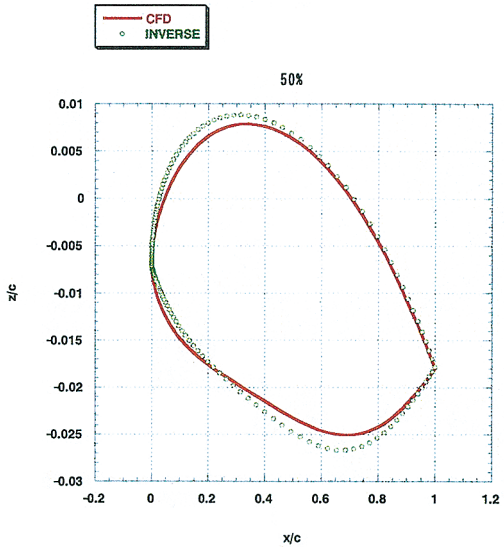

Figure 7. Corresponding geometry of CFD analysis and obtained by inverse method.

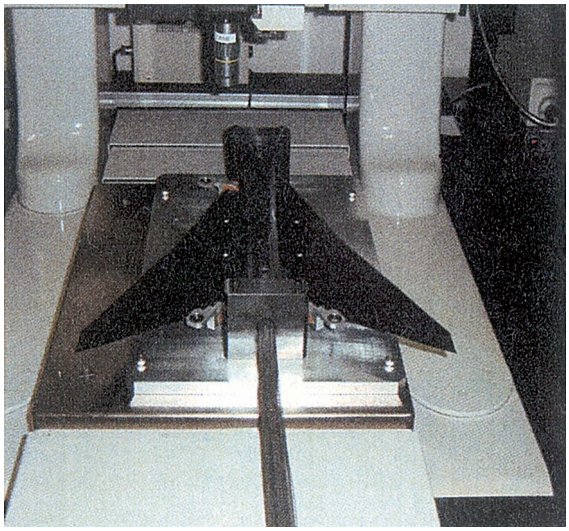

Figure. 8 Three dimensional non-contact measuring device

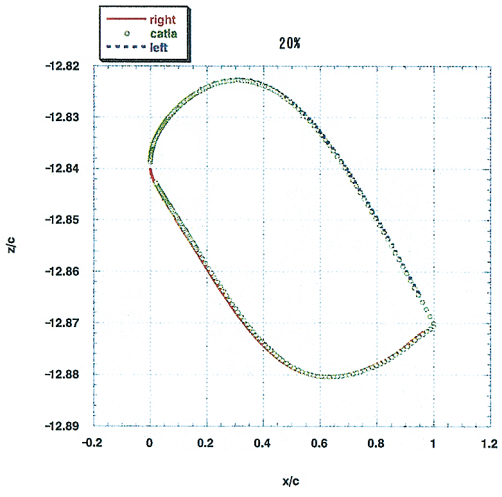

(a) 20% spanwise section

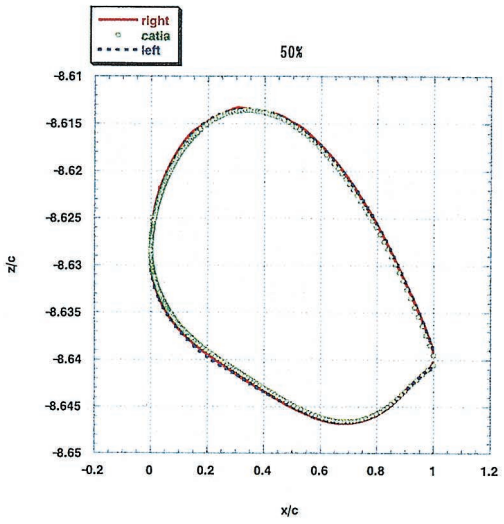

(b) 50% spanwise section

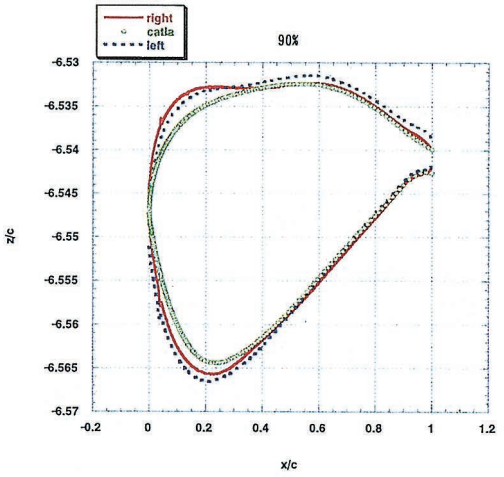

(c) 90% spanwise section

Figure 9. Measurement results

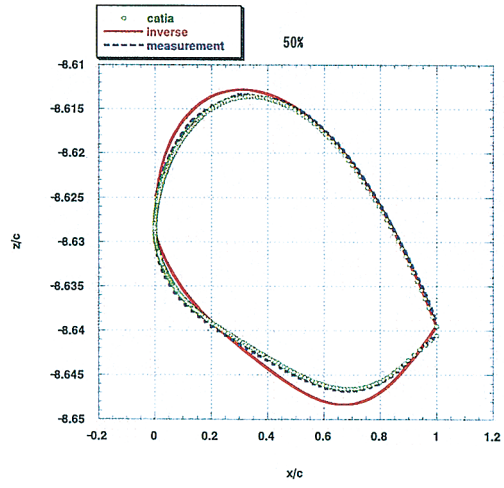

Figure 10. Comparison of geometry of CATIA, inverse estimation, and three-dimensional measurement